Electronic Supporting Information (ESI)

NIR light-driven deflagration of energetic copper complexes through photothermal effect

Bin Tan,[a] Chao Chen,[b] Yun-Rui Chen,[a] Jie Zhang*[a] and Guo-Yu Yang[a]

[a]MOE Key Laboratory of Cluster Science, Beijing Key Laboratory of Photoelectronic/Electrophotonic Conversion Materials, School of Chemistry and Chemical Engineering, Beijing Institute of Technology, Beijing 102488, P. R. China

E-mail: zhangjie68@bit.edu.cn

[b]Fujian Institute of Research on the Structure of Matter, the Chinese Academy of Sciences, Fuzhou, Fujian 350002, P. R. China

Table S1 The crystal data and structure refinements for **1-3**.

	1	**2**	**3**
Empirical formula	$C_{28}H_{16}Cl_4Cu_2N_8O_{28}$	$C_{21}H_{13}Cl_3Cu_2N_6O_{22}$	$C_7H_8Cu_2N_2O_{11}$
Formula weight	1181.37	934.80	423.23
Crystal system	Monoclinic	Triclinic	Triclinic
Space group	$P2_1/c$	P-1	P-1
a/Å	8.1283(7)	8.1404(3)	6.9081(4)
b/Å	23.4063(19)	14.6857(8)	8.0731(5)
c/Å	11.9716(10)	14.8527(7)	11.5005(8)
α/°	90	111.203(5)	105.515(6)
β/°	108.067(9)	104.809(4)	92.979(5)
γ/°	90	99.771(4)	97.637(5)
V/Å^3	2165.3(3)	1531.23(14)	609.95(7)
Z	2	2	2
D_c/g·cm^3	1.812	2.027	2.304
μ/mm^{-1}	1.337	1.760	5.005
F(000)	1180	932	420
No. of reflections measured	20739	15526	4908
No. of independent reflections	5348	6251	2517
No. of parameters	316	508	218
$GOOF$	1.043	1.027	1.032
R_{int}	0.0300	0.0271	0.0282
R_1, wR_2 [I>2σ(I)][a, b]	0.0565, 0.1459	0.0305, 0.0726	0.0327, 0.0860
R_1, wR_2 (all data)	0.0760, 0.1610	0.0394, 0.0774	0.0388, 0.0912
Largest diff. peak and hole /e Å^{-3}	1.108, -0.782	0.386, -0.457	0.453, -0.730

[a]$R_1 = \sum \| F_o | - | F_c \| / \sum | F_o |$, [b]$wR_2 = [\sum w(F_o^2-F_c^2)^2/\sum w(F_o^2)^2]^{1/2}$

Table S2 Bond lengths [Å] and angles [deg] for **1**.

Cu(1)-O(1)	1.959(2)	Cu(1)-O(2)#1	1.969(2)
Cu(1)-O(8)#1	1.962(3)	Cu(1)-O(1W)	2.138(4)
Cu(1)-O(7)	1.963(3)	Cu(1)-Cu(1)#1	2.6544(9)
O(1)-Cu(1)-O(8) #1	90.28(12)	O(7)-Cu(1)-O(2)#1	88.84(12)
O(1)-Cu(1)-O(7)	89.60(13)	O(1)-Cu(1)-O(1W)	97.79(14)
O(8)#1-Cu(1)-O(7)	167.87(13)	O(8)#1-Cu(1)-O(1W)	99.40(16)
O(1)-Cu(1)-O(2)#1	168.02(11)	O(7)-Cu(1)-O(1W)	92.63(16)
O(8)#1-Cu(1)-O(2)#1	88.77(12)	O(2)#1-Cu(1)-O(1W)	94.15(14)

Symmetry transformations used to generate equivalent atoms: #1 -x+1,-y+1,-z+1

Table S3 Bond lengths [Å] and angles [deg] for **2**.

Cu(1)-O(1)	1.9425(14)	Cu(2)-O(3)	1.9353(17)
Cu(1)-O(9)#1	1.9490(16)	Cu(2)-O(8)	1.9417(16)
Cu(1)-O(2)	1.9660(17)	Cu(2)-O(1)	1.9674(15)
Cu(1)-O(1W)	1.9852(16)	Cu(2)-O(1)#1	1.9691(16)
Cu(1)-O(2W)	2.336(2)	Cu(2)-O(14)	2.3909(17)
O(1)-Cu(1)-O(9)#1	95.33(7)	O(3)-Cu(2)-O(8)	86.09(7)
O(1)-Cu(1)-O(2)	95.35(6)	O(3)-Cu(2)-O(1)	93.89(7)
O(9)#1-Cu(1)-O(2)	169.31(6)	O(8)-Cu(2)-O(1)	164.64(8)
O(1)-Cu(1)-O(1W)	170.76(7)	O(3)-Cu(2)-O(1)#1	175.89(8)
O(9)#1-Cu(1)-O(1W)	84.84(7)	O(8)-Cu(2)-O(1)#1	95.28(7)
O(2)-Cu(1)-O(1W)	84.70(7)	O(1)-Cu(2)-O(1)#1	83.76(7)
O(1)-Cu(1)-O(2W)	93.00(7)	O(3)-Cu(2)-O(14)	96.00(7)
O(9)#1-Cu(1)-O(2W)	91.53(9)	O(8)-Cu(2)-O(14)	100.50(7)
O(2)-Cu(1)-O(2W)	87.43(9)	O(1)-Cu(2)-O(14)	94.78(6)
O(1W)-Cu(1)-O(2W)	96.23(8)	O(1)#1-Cu(2)-O(14)	87.57(6)

Symmetry transformations used to generate equivalent atoms: #1 -x+1,-y+2,-z+1

Table S4 The hydrogen bonding data for **2**.

D-H···A	d(D-H)/Å	d(H···A)/Å	d(D···A)/Å	<(DHA)/°
O(1)-H(1)···O(14)#1	0.810(10)	2.62(2)	3.032(2)	113(2)
O(1)-H(1)···O(15)#1	0.810(10)	1.834(14)	2.608(2)	159(3)
O(1W)-H(1WA)···O(14)#2	0.825(10)	1.859(13)	2.663(2)	165(3)
O(1W)-H(1WB)···O(3W)	0.821(10)	1.966(15)	2.741(3)	157(2)
O(2W)-H(2WA)···O(18)#3	0.817(10)	2.293(18)	3.071(3)	159(4)
O(2W)-H(2WB)···O(15)#1	0.819(10)	2.05(2)	2.737(3)	141(3)
O(3W)-H(3WA)···O(5)#6	0.821(10)	2.38(4)	2.996(3)	132(4)
C(3)-H(3)...O(7)#4	0.93	2.43	3.290(3)	154.0
C(10)-H(10)...O(12)#5	0.93	2.46	3.341(3)	157.1
C(14)-H(14)...O(14)#4	0.93	2.44	3.359(3)	168.0
C(17)-H(17)...O(9)#5	0.93	2.49	3.415(3)	172.5
C(21)-H(21)...O(17)#4	0.93	2.55	3.456(3)	166.3

Symmetry transformations used to generate equivalent atoms: #1 -x+1,-y+2,-z+1; #2 -x,-y+2,-z+1; #3 x,y,z+1; #6 -x,-y+1,-z+1

Table S5 Bond lengths [Å] and angles [deg] for **3**.

Cu(1)-O(3)	1.928(2)	Cu(2)-O(2)	1.938(2)
Cu(1)-O(1)	1.9531(19)	Cu(2)-O(4)	1.944(2)
Cu(1)-O(1W)	1.961(2)	Cu(2)- O(2)#2	1.950(2)
Cu(1)-O(1)#1	1.9649(19)	Cu(2)-O(1)	1.971(2)
Cu(1)-O(2W)	2.368(3)	Cu(2)-O(2W)	2.410(2)
Cu(1)-Cu(1)#1	2.9534(8)	Cu(2)-Cu(2)#2	2.9268(8)
O(3)-Cu(1)-O(1)	98.64(8)	O(2)-Cu(2)-O(4)	90.10(9)
O(3)-Cu(1)-O(1W)	89.45(9)	O(2)-Cu(2)-O(2)#2	82.33(9)
O(1)-Cu(1)-O(1W)	170.42(9)	O(4)-Cu(2)-O(2) #2	169.19(9)
O(3)-Cu(1)-O(1)#1	171.68(9)	O(2)-Cu(2)-O(1)	170.25(9)
O(1)-Cu(1)-O(1)#1	82.16(8)	O(4)-Cu(2)-O(1)	93.56(9)
O(1W)-Cu(1)-O(1)#1	89.09(9)	O(2)#2-Cu(2)-O(1)	92.75(8)
O(3)-Cu(1)-O(2W)	90.50(9)	O(2)-Cu(2)-O(2W)	108.73(10)
O(1)-Cu(1)-O(2W)	81.84(8)	O(4)-Cu(2)-O(2W)	88.92(9)
O(1W)-Cu(1)-O(2W)	103.34(9)	O(2)#2-Cu(2)-O(2W)	100.78(9)
O(1)#1-Cu(1)-O(2W)	97.81(8)	O(1)-Cu(2)-O(2W)	80.40(8)

Symmetry transformations used to generate equivalent atoms: #1 -x,-y+1,-z; #2 -x,-y,-z

Table S6 The hydrogen bonding data for **3**.

D-H···A	d(D-H)/Å	d(H···A)/Å	d(D···A)/Å	<(DHA)/°
O(1W)-H(1WA)···O(2)#3	0.817(10)	1.92(2)	2.651(3)	149(4)
O(1W)-H(1WB)···O(5)#4	0.819(10)	2.25(3)	2.871(3)	133(3)
O(2W)-H(2WA)···O(1W)#5	0.816(10)	2.39(3)	3.050(3)	139(3)
O(1)-H(1)···O(7)#6	0.801(18)	1.82(2)	2.614(3)	168(4)
O(2)-H(2)···O(8)#7	0.806(19)	2.13(3)	2.878(3)	154(4)

symmetry transformations used to generate equivalent atoms: #3 x,y+1,z; #4 -x+1,-y+2,-z+1; #5 -x+1,-y+1,-z; #6 -x,-y+1,-z+1; #7 -x,-y,-z+1

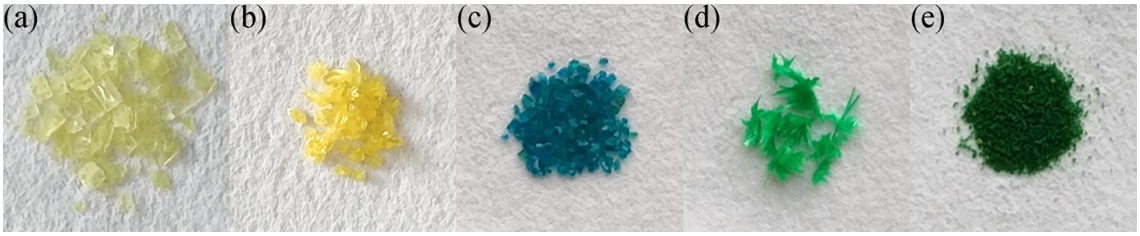

Fig. S1 The photographs of HDNB-Cl (a), HDNB-OH (b) and crystals for **1** (c), **2** (d) and **3** (e).

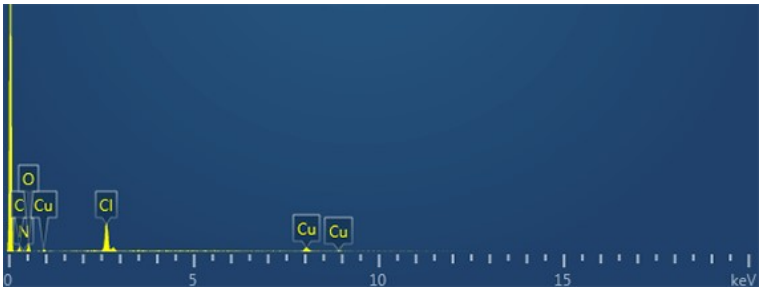

Fig. S2 EDS of **1** shows Cl in the structure.

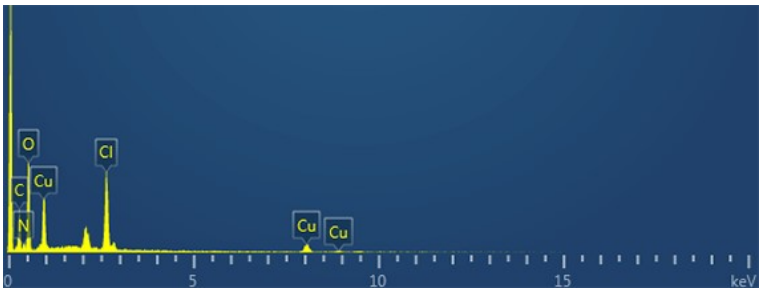

Fig. S3 EDS of **2** shows Cl in the structure.

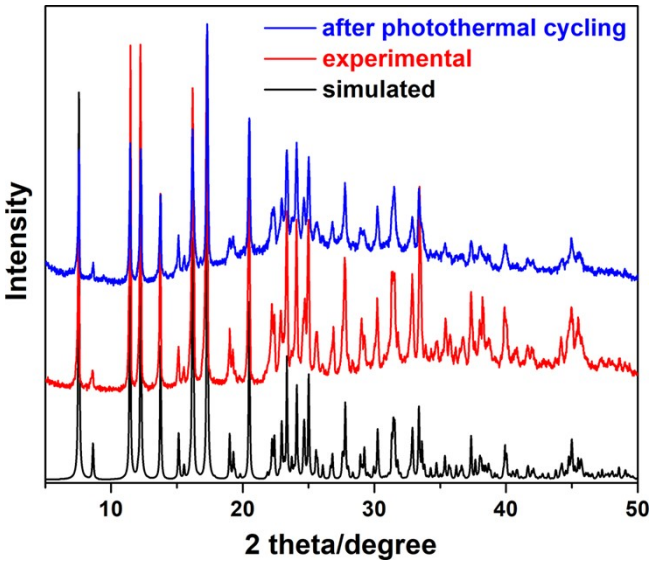

Fig. S4 PXRD patterns of **1**.

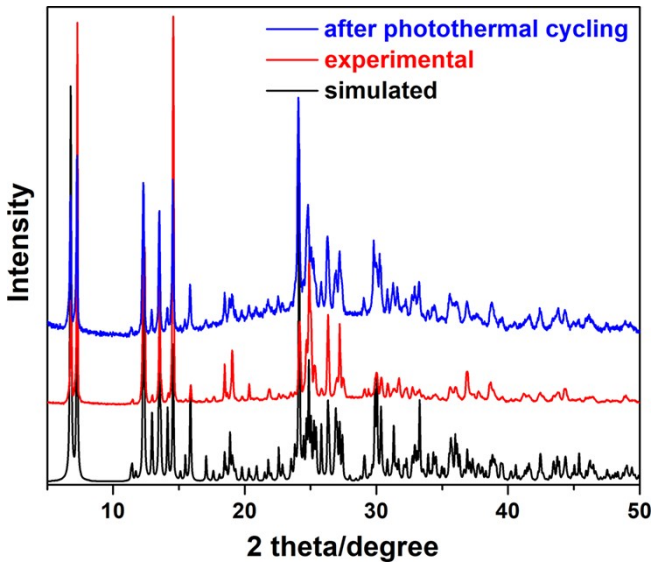

Fig. S5 PXRD patterns of **2**.

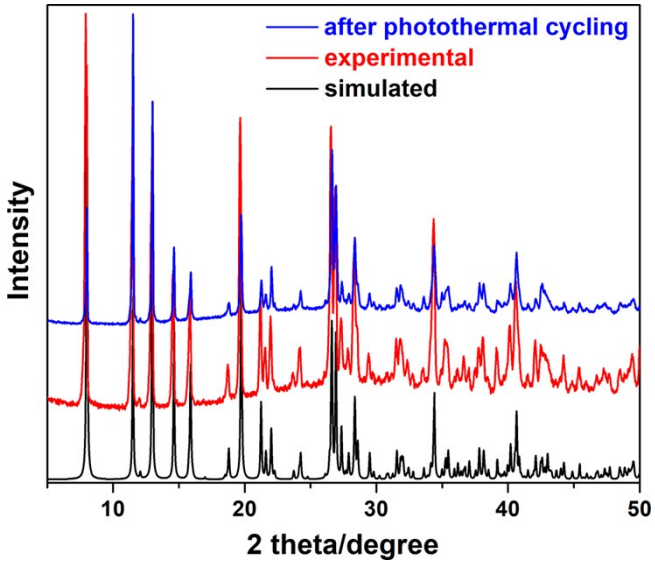

Fig. S6 PXRD patterns of **3**.

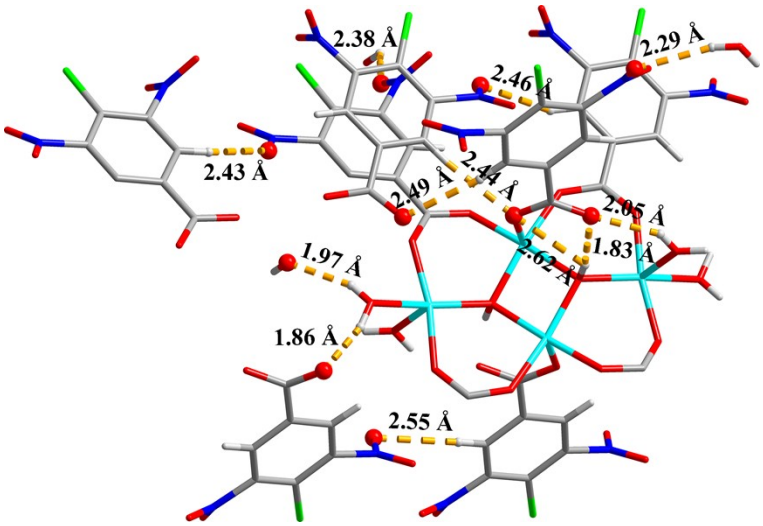

Fig. S7 The hydrogen bonding interactions in **2**. H···O distances are marked.

There are two types of hydrogen bonds in **2**, which are O-H···O hydrogen bonds [O (terminal water molecule)-H···O (carboxylate oxygen) hydrogen bonds (H···O separations: 1.86 and 2.05 Å), O (terminal water molecule)-H···O (nitro group) hydrogen bonds (H···O separations: 2.29 Å), O (terminal water molecule)-H···O (free water molecule) hydrogen bonds (H···O separations: 1.97 Å), O (μ_3-OH anion)-H···O (carboxylate oxygen) hydrogen bonds (H···O separations: 1.83 and 2.62 Å), and O (free water molecule)-H···O (nitro group) hydrogen bonds (H···O separations: 2.38 Å)]; the extensive C-H···O hydrogen bonds [C (benzene ring)-H···O (carboxylate oxygen) hydrogen bonds (H···O separations: 2.44 and 2.49 Å), C (benzene ring)-H···O (nitro group) hydrogen bonds (H···O separations: 2.43, 2.46 and 2.55 Å)].

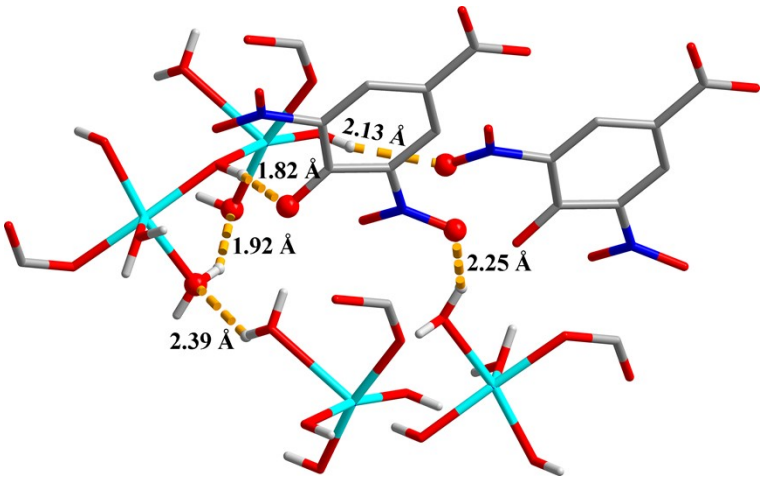

Fig. S8 The hydrogen bonding interactions in **3**. H···O distances are marked.

There are abundant O-H···O hydrogen bonds in compound **3**, that are [O (terminal water molecule)-H···O (μ_2-OH anion) hydrogen bonds (H···O separations: 1.92 Å), (O (terminal water molecule)-H···O (nitro group) hydrogen bonds (H···O separations: 2.25 Å), O (bridging water molecule)-H···O (terminal water molecule) hydrogen bonds (H···O separations: 2.39 Å), O (μ_3-OH anion)-H···O (phenolic hydroxyl group) hydrogen bonds (H···O separations: 1.82 Å), and O (μ_2-OH anion)-H···O (nitro group) hydrogen bonds (H···O separations: 2.13 Å)] (Fig. S8).

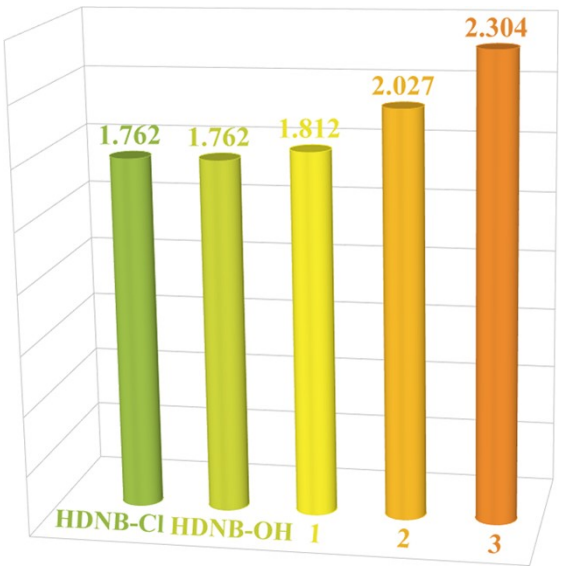

Fig. S9 Density comparison of ligands and compounds **1-3**.

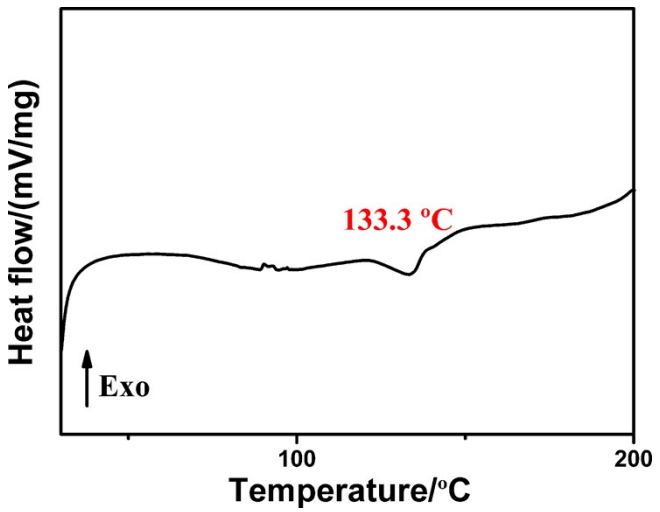

Fig. S10 A zoom in view of the endothermic peak in **1**.

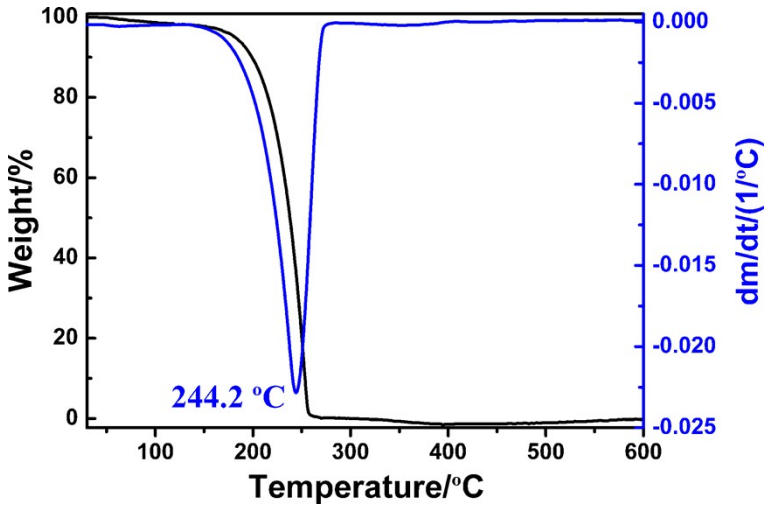

Fig. S11 TG and DTG curves of HDNB-Cl.

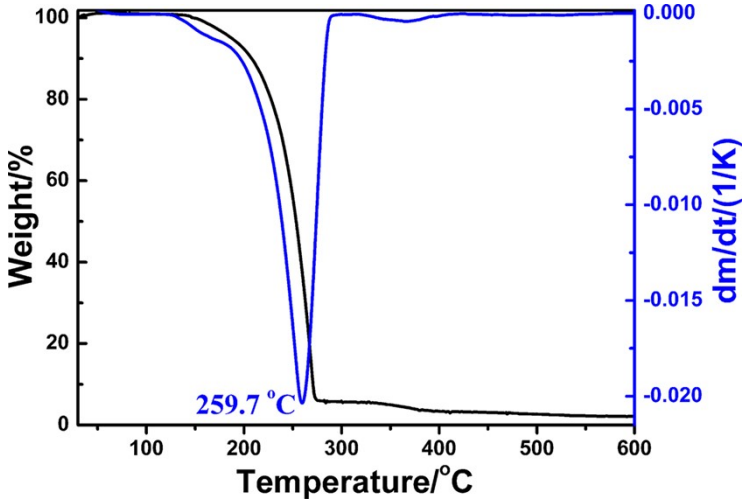

Fig. S12 TG and DTG curves of HDNB-OH.

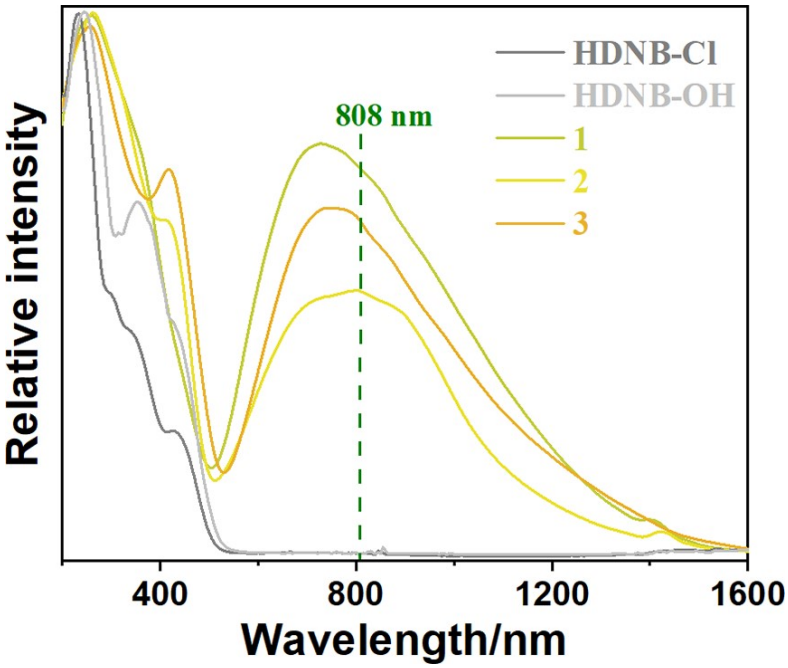

Fig. S13 Solid state UV-vis spectra of ligands and compounds **1**-**3**.

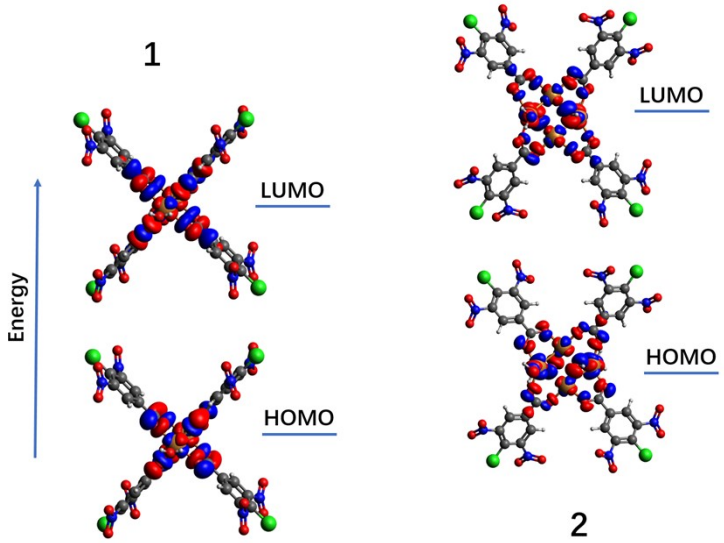

Fig. S14 The energies and compositions of HOMO and LUMO of **1** and **2**.

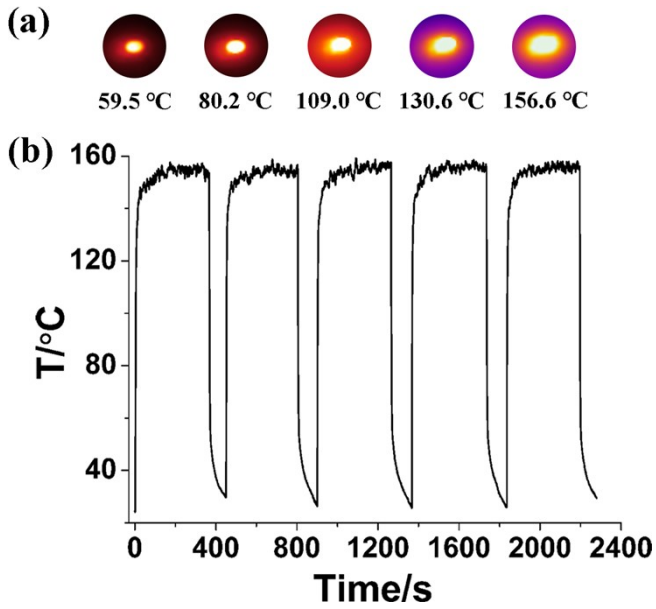

Fig. S15 (a) IR thermal images of **1** under different NIR laser intensities (0.3, 0.5, 0.75, 1.0 and 1.25 W·cm^{-2}). (b) Photothermal cycling curve of **1** performed at 1.25 W·cm^{-2} laser intensity.

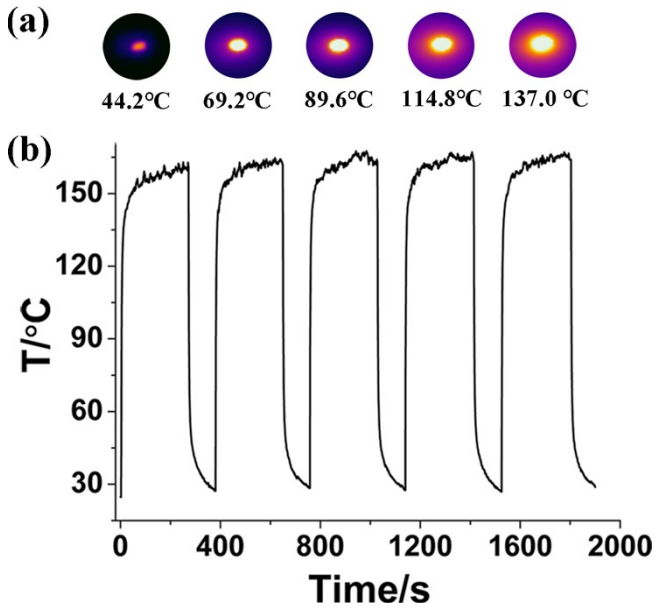

Fig. S16 (a) IR thermal images of **2** under different NIR laser intensities (0.3, 0.5, 0.75, 1.0 and 1.25 W·cm^{-2}). (b) Photothermal cycling curve of **2** performed under 1.5 W·cm^{-2} laser intensity.

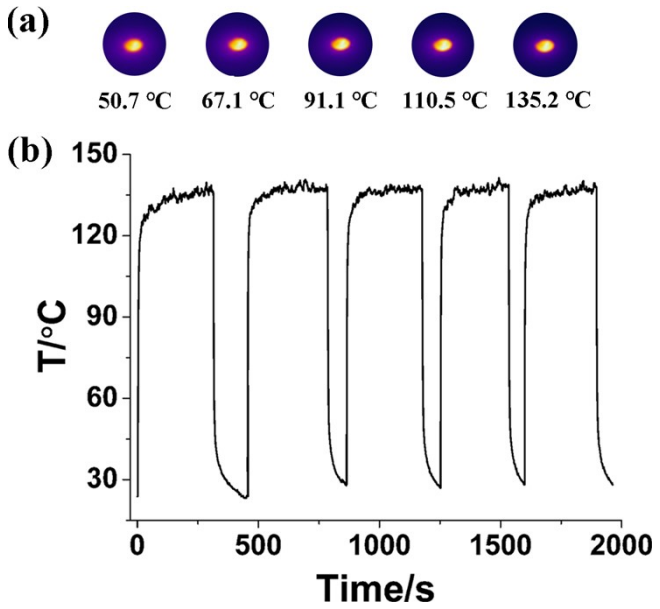

Fig. S17 (a) IR thermal images of **3** under different NIR laser intensities (0.3, 0.5, 0.75, 1.0 and 1.25 W·cm^{-2}). (b) Photothermal cycling curve of **3** at 1.25 W·cm^{-2} laser intensity.

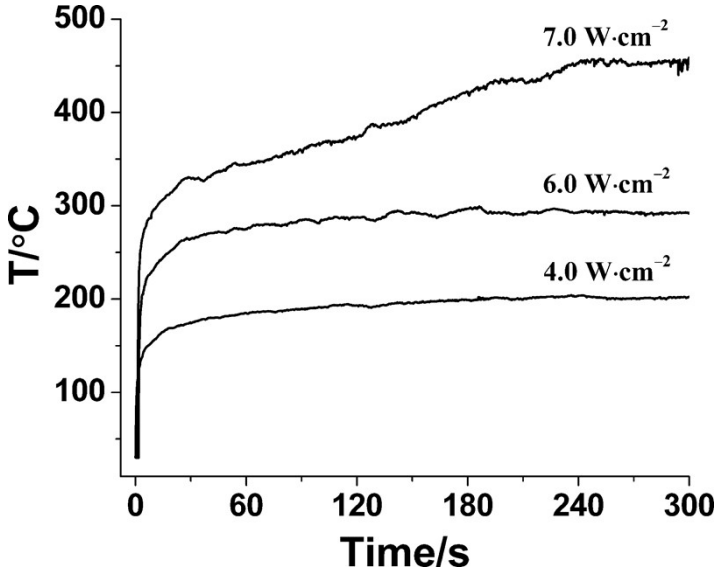

Fig. S18 Photothermal conversion curves of **3** at different NIR laser intensities from 4 to 7 W·cm^{-2}.

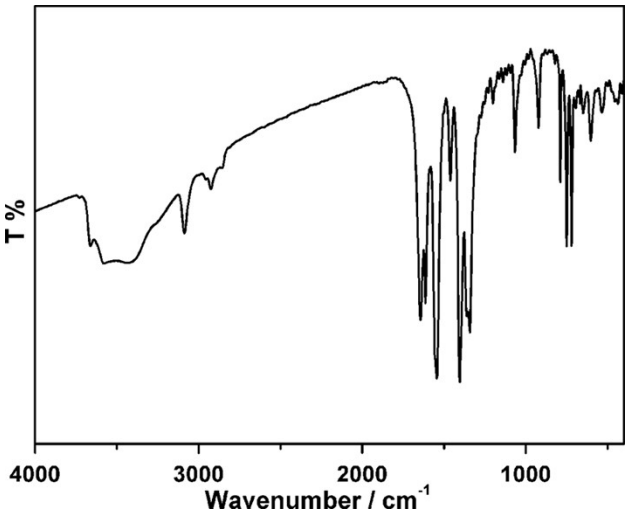

Fig. S19 IR spectrum of compound **1**.

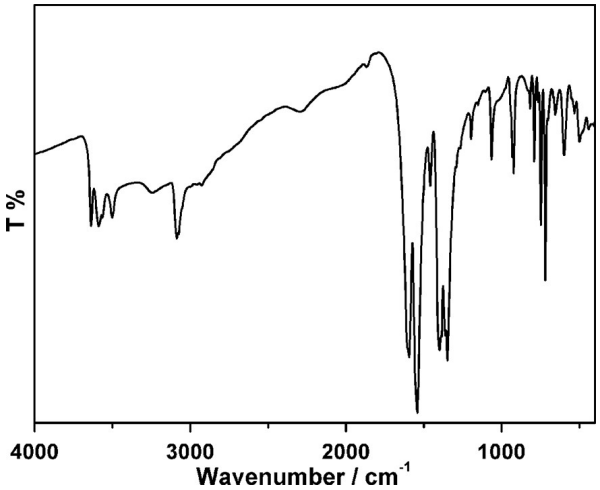

Fig. S20 IR spectrum of compound **2**.

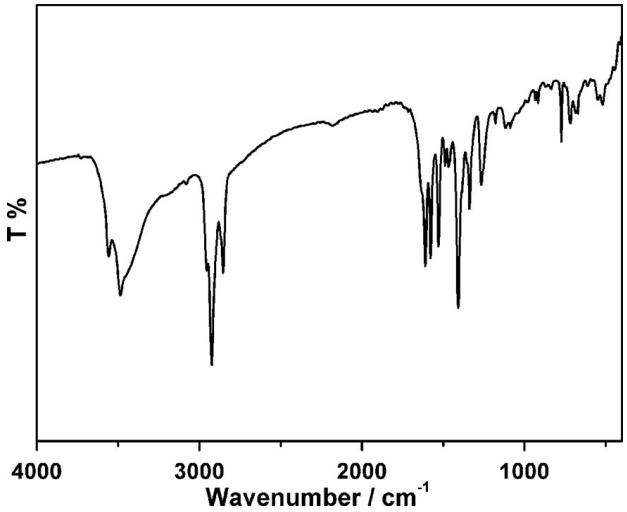

Fig. S21 IR spectrum of compound **3**.